INSTITUTE OF PHYSICS PUBLISHING METROLOGIA
Metrologia **42** (2005) S31–S42 doi:10.1088/0026-1394/42/3/S05

The classical caesium beam frequency standard: fifty years later

Jacques Vanier[1] **and Claude Audoin**[2]

[1] Département de physique, Université de Montréal, Montréal, Québec, H3C 3J7, Canada
[2] BNM-SYRTE, Observatoire de Paris, 61 Avenue de l'Observatoire, 75014 Paris, France

Received 16 December 2004
Published 7 June 2005
Online at stacks.iop.org/Met/42/S31

Abstract
The caesium beam frequency standard using the separated oscillatory field technique proposed by Ramsey in 1950 has seen intensive development over the last fifty years. Its practical implementation as a primary time standard made possible the realization of the second with a precision better than that obtained by means of astronomical measurements and provided the basis for its redefinition in terms of atomic properties in 1967. This paper describes the basic principles underlying the operation of such atomic standards, reviews the progress made during the last fifty years since its invention, and provides an update on the state-of-the-art accuracy and frequency stability achieved today in this field.

1. Introduction

After the first implementation by Essen and Parry [1] of an atomic frequency standard using a Cs beam excited by means of the separated oscillatory field approach proposed by Ramsey [2], a period of intense research and development followed, in national laboratories as well as in industry. National laboratories were interested mainly in accuracy while industry's interest was concentrated on size and frequency stability. Research in national laboratories was crowned by such success that a new definition of the unit of time in terms of an atomic property, the hyperfine frequency of Cs in its ground state, was established in 1967 and led to the new SI second [3]. On the other hand, development in industry resulted in systems with excellent frequency stability and small size, leading to the use of Cs beam frequency standards in many advanced applications, such as time-keeping, digital communication, high accuracy metrology, positioning, geodesy and advanced navigation systems, including GPS, Glonass and Loran C.

As mentioned in other papers of this special issue, in such frequency standards the frequency is derived from an internal property of the caesium atom, the magnetic interaction of the unpaired electron with the nucleus causing a splitting of the ground state into two separate states called hyperfine levels. The separation of these two levels in Cs corresponds to a resonance frequency close to 9.2 GHz. The concept of using an atomic property was based essentially on the expectation that the resulting resonance frequency would be independent of space and time—provided that relativistic effects have been properly accounted for—and independent of environmental perturbations, leading to the possibility of reproducing this frequency with a high level of accuracy. It was also expected that with a proper development of supporting electronics, systems based on this concept would provide frequency stability greater than that provided by quartz oscillators used at large in applications requiring accurate timing.

In the classical room temperature Cs beam frequency standard, a beam of atoms is formed in an oven and allowed to drift freely in high vacuum into an interaction region formed by a microwave structure called the Ramsey cavity [4]. The structure is generally machined or realized out of a piece of X band waveguide bent into a U shape. This arrangement creates two short microwave interaction regions of length l, separated by a relatively large distance L, and having almost the same phase. In their trajectory, the atoms traverse the first interaction region, are exposed to the microwave field for a short time, evolve freely over the distance L, then enter the second interaction region and are exposed to the same microwave field. The resonance frequency of the Cs atoms is determined using the well-known technique of magnetic resonance [5, 6]. In this technique, transitions are excited between the two levels whose energy difference corresponds to the resonance frequency and the effect of these transitions on the ensemble of atoms is detected through changes in the population of the levels. The advantage of the Ramsey structure over the single cavity approach is that interferences take place between the excitation in the two interaction regions, leading to the so-called 'Ramsey fringes', and resulting in a

 © 2005 BIPM and IOP Publishing Ltd Printed in the UK

narrowing of the resonance feature by a factor of the order of L/l.

In thermal equilibrium, however, the ground state energy levels are essentially all equally populated and since the transition probability from the lower level to the upper one is equal to the transition probability from the upper level to the lower one, no net effect results. It is thus essential that before they enter the Ramsey interaction region, a difference of population be created between the two energy levels in question. This requirement has led to the development of two radically different approaches in the implementation of the Cs beam frequency standard.

One approach uses intense magnetic field gradients [7] to separate spatially the beam atoms in the lower state from those in the upper state. By simple collimation the desired atoms can then be directed in the interaction region where transitions are excited. The process is called magnetic state selection. In such an approach, the detection is done also through magnetic state selection by directing atoms that have made a transition to a hot wire ionizer usually followed by an electron multiplier. The Cs atom has an advantage over several other candidates in that its ionization energy is relatively low (3.9 eV) and a hot tungsten wire provides sufficient energy for the ionization process.

The other approach uses optical radiation as a means of populating one level at the expense of the other. The technique is called optical pumping [8]. It is possible through such a process to send almost all atoms into one of the two levels. The technique is also used for the detection process. It has an advantage over the previous one using magnets in that strong magnetic fields close to the interaction region are avoided and ionization of the Cs atoms is no longer required. Furthermore, the velocity dispersive deflection of atoms in a thermal beam interacting with light is negligible. The atoms are thus more efficiently used in this approach.

In practice, however, the atoms are not totally free of the environment. For example, a magnetic field along the axis of the beam is required to provide a quantization axis to the resonance excitation. This field shifts the energy levels and consequently changes the resonant frequency of the atoms by a relatively large amount. The atoms travel at a velocity that depends on temperature. Although the first-order Doppler effect is avoided through the use of a microwave cavity and standing waves, the resonant frequency of the atoms is altered by the so-called second-order Doppler effect originating from the phenomenon of time dilation of relativity. Another shift may also be caused by small imperfections in the Ramsey cavity structure. If a small unwanted phase shift exists between the two interaction regions, the resonant frequency of the atoms is altered. Another small shift may be the light shift introduced by the fluorescence created by the state selection and detection when the optical pumping technique is used. Offsets may also be introduced indirectly by the electronics system that locks the oscillator used to excite the Ramsey structure to the atomic resonance. As is readily observed, some of these shifts are inherent to the atomic ensemble while others are introduced by either the state selection or the resonance excitation itself. It is recognized that these various shifts and offsets may have an effect on the frequency stability as well as on the accuracy of the frequency standards implemented according to the technique just described.

In this paper we will review the progress made in the implementation of the Cs beam frequency standards using the two approaches, magnetic selection and optical pumping. This paper will concentrate on the so-called classical caesium beam frequency standards operating at room temperature. Recent developments using laser-cooled Cs and Rb atoms leading to the atomic fountain concept are the subject of other papers of this special issue of *Metrologia*.

We will review phenomena that appear to have a detectable effect on the atomic resonance frequency. We will do this in relation to concepts such as accuracy, frequency stability, and functionality. We will summarize the results of various implementations in national laboratories. We will also mention briefly the results obtained in the implementation of field-used commercial Cs beam frequency standards.

Several papers and texts have been written that summarize to various degrees the operation and the progress made in this field [9–12]. This paper is a concise update of those texts and the bibliography is aimed at being a guide to interested readers who wish to pursue their readings.

2. Implementation of the classical Cs beam frequency standard

2.1. Some basic considerations

The choice of the Cs atom for the implementation of a frequency standard has resulted from the considerable accumulation of knowledge on that atom over the years and from the several advantages that it provides over other candidates. In particular, Cs has a single stable isotope, ^{133}Cs, and is relatively abundant in nature. Its melting point is around 28.4 °C. Its vapour pressure is such that it is possible to obtain an intense atomic beam from an oven at a temperature of about 100 °C. Its ionization energy is 3.9 eV, making it easy to detect by conventional ionizing processes with a hot wire detector. Finally, Cs has a ground state hyperfine frequency falling in the X band, a microwave region that has known extensive development, and making possible small structures such as that required in the Ramsey cavity concept.

The Cs nuclear spin is 7/2 and its ground state consists of two hyperfine levels $F = 3$ and $F = 4$. The structure consists of two manifolds of 7 and 9 levels, respectively, as shown in figure 1 as a function of the magnetic induction $\boldsymbol{B}$. The transition of interest is that from level $F = 4$, $m_F = 0$ to level $F = 3$, $m_F = 0$. Its frequency has been defined as 9 192 631 770 Hz [3].

2.2. Approach using magnetic state selection

A conceptual diagram of the classical Cs beam frequency standard using magnetic state selection is shown in figure 2. Magnets A and B are generally dipole magnets and create an intense inhomogeneous field in which atomic trajectories are deflected. The deflection is caused by the tendency of atoms to seek states of low potential energy. Consequently, according to figure 1 atoms having higher energy in high magnetic fields are deflected to regions of low magnetic field in order to lower their potential energy. Similarly, atoms having lower energies in high magnetic fields seek regions of high magnetic field for the same reason. Selection is accomplished by means

of magnet A whose orientation is such as to force atoms in level $F = 4$, $m_F = 0$ to pass through the Ramsey microwave cavity and reach the second deflecting magnet B. Atoms in the other $F = 3$, $m_F = 0$ level are eliminated from the beam by appropriate collimating. The analysis of the beam composition is done by a combination of magnet B called the analyser and a hot wire ionizer followed usually by an electron multiplier. The atoms traverse the Ramsey cavity where they are submitted to an electromagnetic field of angular frequency ω in the two interaction regions. If this frequency corresponds to the hyperfine angular frequency ω_{hf}, atoms are transferred from the $F = 4$, $m_F = 0$ level to the $F = 3$, $m_F = 0$ level and at the exit of the cavity the beam is composed of atoms in that state. These atoms are deflected by magnet B so as to hit the detector, while those atoms remaining in the level $F = 4$, $m_F = 0$ are deflected away from the detector. Consequently, the detector signal output is a maximum when the frequency is exactly that of the hyperfine transition. It is worth mentioning that the role of atoms in level $F = 4$, $m_F = 0$ and of atoms in level $F = 3$, $m_F = 0$ can be inverted without affecting the operation of the system.

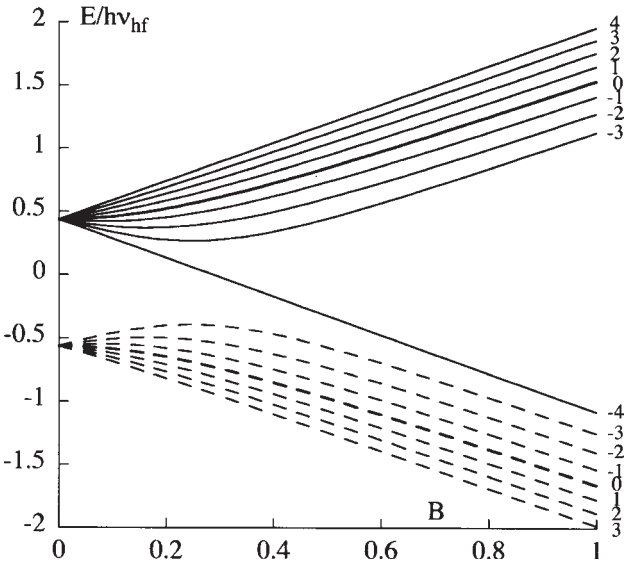

Figure 1. Ground state energy level manifold of the caesium atom as a function of the magnetic induction $\boldsymbol{B}$ in tesla.

2.3. Approach using optical pumping

With the advent of solid-state diode lasers with narrow spectra, it has become possible to excite specific narrow optical transitions in alkali metal atoms, connecting a single hyperfine level of the ground state to either of the excited $P_{1/2}$ or $P_{3/2}$ states. In such a process, it is possible to populate a given ground state hyperfine level at the expense of the other. The process has been given the name optical pumping [8].

The lower energy levels of the Cs atom are illustrated in figure 3. Several optical pumping schemes are possible. In one of them, atoms are excited from level $F = 4$ of the ground state to level $F' = 3$ of the excited state. The lifetime of atoms in the excited state is of the order of 30 ns and they fall back to the two hyperfine levels of the ground state with nearly equal probabilities. This process thus tends to increase the population of level $F = 3$ at the expense of level $F = 4$. It can thus be used to select atoms in that energy level. Similarly, at the exit of the Ramsey interaction region the same technique can be used to analyse the composition of the beam in the various levels. In that case, a particular transition is again excited, for example $F = 4$ to $F' = 5$, and the fluorescence emitted by the atoms upon decay to the ground state is used as a measure of the population in level $F = 4$ and is a measure of the number of atoms that have made a transition in the

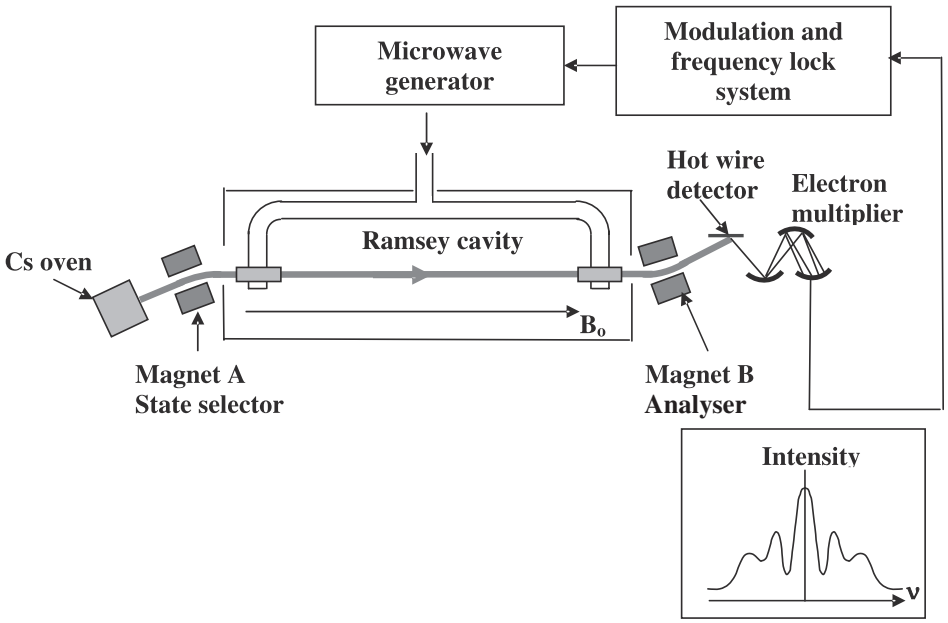

Figure 2. Simplified conceptual diagram of the Cs beam frequency standard using magnetic state selection. The inset shows the shape of the resonant signal observed when the frequency-lock loop is open and the microwave frequency is scanned slowly over the atomic hyperfine resonance. Although in the figure the magnetic induction is shown parallel to the beam direction, in practice it is very often made perpendicular to the beam.

Ramsey interaction region. This approach thus avoids the use of selector magnets. It is illustrated in figure 4. It was first implemented in a Rb beam with spectral lamps [13] and then refined in a Cs beam through the use of laser diodes [14].

We will not give the details of the calculation involved in the optical pumping state selection. The reader is referred to [9] for details. It is sufficient to say that one advantage of the approach lies in the fact that the system is highly symmetrical and avoids magnetic inhomogeneities that can be present when magnetic state selectors are used. The inherent symmetry of the optical pumping state selection results in the absence of asymmetry in the amplitude of the field-dependent transitions and reduces considerably the effect of Rabi and Ramsey pulling that will be discussed later. The Rabi pedestal frequency shift is thus essentially eliminated. On the other hand, in the case of magnetic selection, an offset geometry is required, resulting in a beam velocity distribution different from the normal modified Maxwell distribution. The distribution must thus be deduced from experimental data. In the case of optical pumping the velocity distribution is known and the averaging required in the calculation of the second-order Doppler frequency shift can be done analytically. Furthermore, in the case of optical pumping, it is possible, by means of several laser diodes for pumping and detection, and proper optical geometry, to transfer almost all the atoms to one of the two m_F levels of the ground state [15]. A somewhat better signal to noise ratio is then possible at the detection, leading to improved frequency stability [16]. Its limitation by the frequency noise of the laser used for state selection has been evaluated [17].

It should be mentioned that since in the Ramsey cavity approach, the microwave field is applied at two separate regions, the following advantages result:

(1) the width of the central fringe of the resonance pattern is narrowed, being proportional to the inverse of the distance between the two arms of the cavity;
(2) the requirements on the homogeneity of the magnetic field in the interaction region are considerably relaxed;
(3) residual frequency shifts occurring in the interaction region are reduced by the ratio of the length of the individual interaction region to the distance between them;
(4) the atomic beam crosses the arms of the cavity at places where the phase of the microwave magnetic field is constant along the trajectories. Consequently, the first-order Doppler effect is absent.

3. Signal amplitude of the classical Cs beam standard

The effect of the two interaction regions on the state of the atoms can be introduced by conceptually replacing them by two $\pi/2$ pulses, a concept commonly encountered in the field of magnetic resonance [18]. In the first cavity, assuming exact resonance between the microwave field and the hyperfine frequency and an appropriate amplitude, atoms having a given velocity are placed into a superposition state with equal probability of being in either of the two states $F = 4$, $m_F = 0$ and $F = 3$, $m_F = 0$. This is similar to the effect of a $\pi/2$ pulse. These atoms traverse the region between the two fields and evolve in that state with little perturbation apart from the constant magnetic field. They enter the second interaction region with a well determined phase dictated by the phase of the field encountered in the first cavity. Since the field in the second cavity is produced by the same source, the atoms in

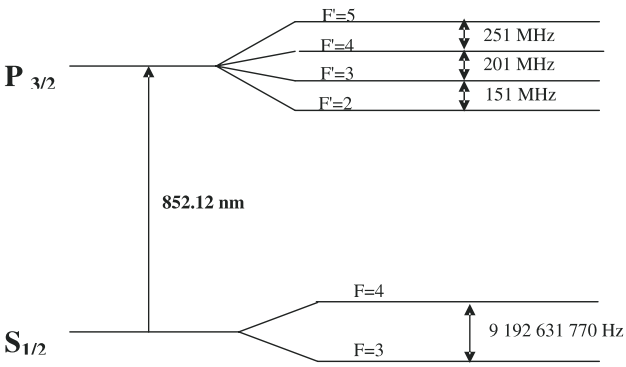

Figure 3. Illustration of the lower states of interest in optical pumping of a Cs beam.

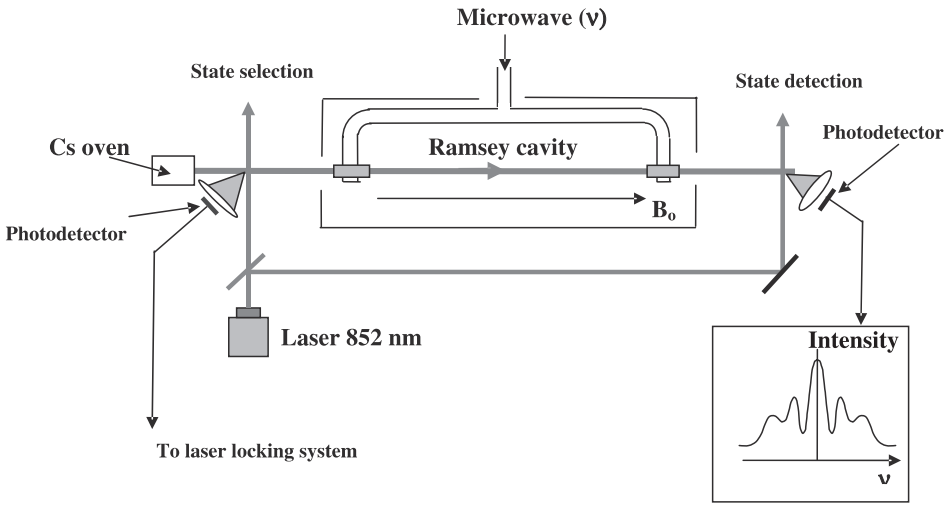

Figure 4. Simplified conceptual diagram of the Cs beam frequency standard using optical pumping for state selection and detection. In the case shown, only one laser is used for both selection and detection. The inset illustrates the amplitude of the fluorescence observed at the detection end when the microwave frequency is swept slowly across the resonance line.

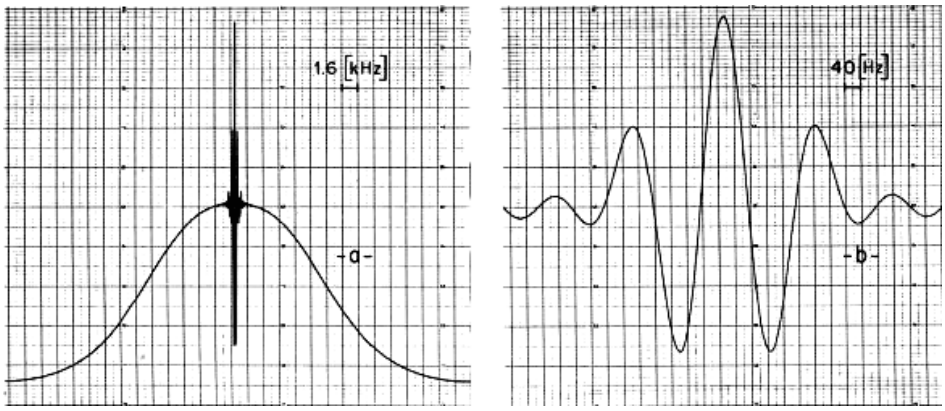

Figure 5. Ramsey fringes observed experimentally in the NRC Cs VI standard [20].

this region undergo an interaction that is phase coherent with the interaction in the first region. Consequently, for a field of the proper amplitude and frequency, the atoms considered pass through the second region experiencing another $\pi/2$ pulse with the same phase as in the first interaction region and find themselves in the $F = 3, m_F = 0$ state.

An important point to realize is the absence of relaxation mechanisms. In the interaction region, the atoms are essentially free except for the time they spend inside the microwave cavity where they are submitted to a microwave field. This is a definite advantage over other types of standards using atom storage in bulbs or cells, either coated internally with an inert substance or containing a buffer gas to prevent wall relaxation. In those approaches a frequency shift is introduced through the storage mechanism. This shift is difficult to determine exactly in practice and prevents those frequency standards from being classified as primary.

The evolution of the populations and of the coherence in the beam may be calculated in several ways, in particular through the wavefunction approach [4] or by means of the density matrix approach [9, 19].

A complete calculation shows that for monochromatic atoms, and assuming $T \gg \tau$ for simplicity, the probability $P(\tau)$ that a transition occurred in the interaction region is given by

$$P(\tau) = \tfrac{1}{2} \sin^2 b\tau (1 + \cos(\omega_{\mu w} - \omega_{hf})T + \Phi), \qquad (1)$$

where τ is the time of interaction of the atom with the microwave field in each interaction region, T is the time spent by the atom between the interaction regions, $\omega_{\mu w}$ is the angular frequency of the microwave radiation in the Ramsey cavity, ω_{hf} is the resonance angular frequency of the atom, and b is the Rabi angular frequency in the interaction region and is a measure of the amplitude of the microwave field. In this expression Φ is the phase difference that exists between the two microwave fields including the effect of asymmetries and cavity losses.

The result just obtained gives rise to interference fringes. The central fringe, which is of particular interest, has a width given by

$$\Delta\omega_{1/2} \cong \frac{\pi}{T}. \qquad (2)$$

The larger the value of T (or space between the two interaction regions), the narrower the line, which is the obvious desired characteristic of a frequency standard. The above calculation was done under the assumption that the atoms in the beam all have the same velocity and spend the same time in the two arms of the cavity. In practice, the beam is composed of atoms travelling at thermal velocities. In optically pumped devices, atoms are distributed over a modified Maxwell distribution. On the other hand, this distribution is greatly altered in the case of state selection by means of magnets. If $f(\tau)$ is the resulting distribution of interaction times τ, then an average over this distribution of the probability $P(\tau)$ must be made:

$$P = \int_0^\infty f(\tau) P(\tau)\, d\tau. \qquad (3)$$

The fringe pattern is smeared out to some extent by the velocity spread. It turns out, however that the central fringe is not much affected by the averaging, if the velocity distribution is sufficiently narrow. A typical experimental result is shown in figure 5. In practice, the frequency of the generator used to excite the atoms in their path is locked to the top of this central fringe by appropriate modulation means as made explicit in figure 2.

For the purpose of comparison, figure 6 shows the resonance pattern obtained in a short optically pumped experimental set-up [21]. Only two fringes on each side of the central fringe are clearly visible since in that case the velocity distribution is very broad.

The approach just described sets the relative phase of the radiation between the two interaction regions of the Ramsey structure equal to zero. However, a different phase difference such as π may be used [22]. In that case, the cosine term in equation (1) changes sign and, as shown in figure 7, the resulting Ramsey interference pattern is inverted relative to the case where the phase is made equal to zero [9]. Then, the transition probability is zero at exact resonance for all atomic velocities. In that case, and considering the transition probability only, there is no background on which the resonance is superimposed. Consequently, the shot noise of the detected atoms is related to the useful part of the resonance pattern only. In contrast, with $\Phi = 0$, the resonance pattern can be considered as having two parts. The lowest one, below the two valleys of the pattern shown in figure 7, does not give any information on the resonance frequency, but brings shot noise that affects the signal-to-noise ratio of the signal

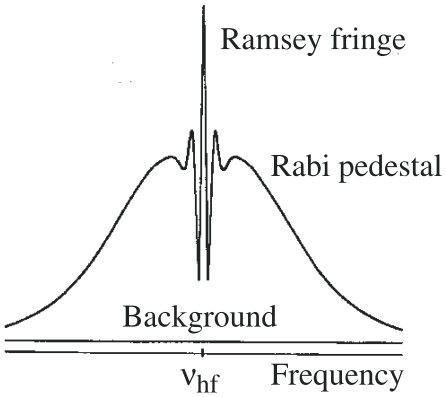

Figure 6. Ramsey pattern obtained in a short optically pumped caesium beam tube. The line width of the central fringe is 500 Hz [21].

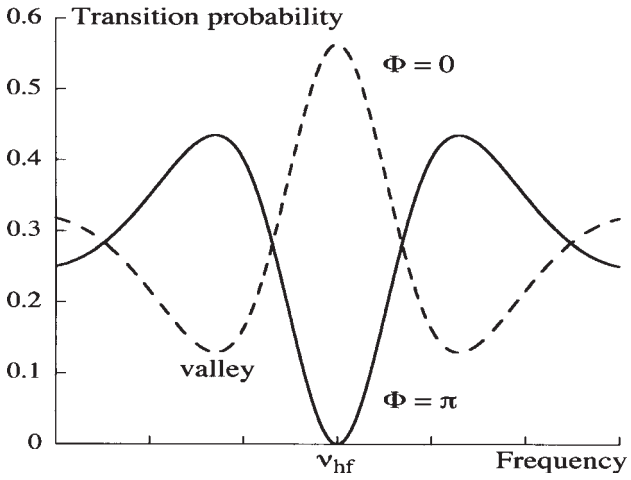

Figure 7. Resonance patterns computed with $\Phi = 0$ and π in an optically pumped caesium beam resonator.

detected. The height of this part is a significant fraction of the resonator response in optically pumped devices where the velocity distribution is broad. Consequently, the configuration with $\Phi = \pi$ is well suited to optically pumped caesium beam resonators [23].

4. Frequency shifts and accuracy

As is evident from the previous analysis, the atoms are relatively free in the beam. There are, however, some physical phenomena that take place causing frequency shifts or offsets. One of the main tasks in the implementation of a primary frequency standard of the type just described is the precise evaluation of these shifts. It is only after such an evaluation that a given standard may be accepted as a representation of the SI unit, the second, which is the main goal in national standards laboratory implementations.

These shifts may be separated into three main groups: those intrinsic to atomic properties, those introduced in the detection of the resonance signal and those introduced in the locking of the generator to the resonance line.

4.1. Frequency shifts associated with physical atomic properties

4.1.1. Magnetic field shift. In a low magnetic field, the shift of the field-independent resonant line of interest with the applied magnetic field is given by the equation [9]

$$\nu = \nu_{hf} + 427.45 \times 10^8 B_0^2 \tag{4}$$

where ν_{hf} is the defined unperturbed hyperfine frequency equal to 9 192 631 770 Hz, and B_0 is the value of the applied magnetic induction in tesla. The field applied may be of the order of $(50–100) \times 10^{-7}$ T. The displacement of the resonance peak is several parts in 10^{-10}. This is the most important shift in the frequency standard and must be determined with an accuracy corresponding to the accuracy desired in the final evaluation. Furthermore, field fluctuations must be minimized for reasons of frequency stability. This constraint forces the use of efficient magnetic shielding around the Ramsey cavity.

4.1.2. Second-order Doppler effect. This shift originates from the time dilation phenomenon of relativity. For an atom of velocity v, the fractional frequency shift is given by the equation

$$\frac{\Delta\nu_{D2}}{\nu_{hf}} = -\frac{v^2}{2c^2}, \tag{5}$$

where c is the speed of light. In the beam, the velocities are spread over a relatively large range and this shift must be averaged over the velocity distribution. It is of the order of -1×10^{-13} or less. It is possible to design state selector magnets such that they select low velocity atoms within a narrow range [24]. Recent development in laser cooling has also shown that it is possible to reduce considerably the average velocity in the beam as well as the velocity spectrum or spread [25, 26]. In practice, it is possible to determine its value through a proper evaluation of the velocity distribution [17, 27–29]. It can be determined to an accuracy better than 1×10^{-14}.

4.1.3. Black body radiation. This effect is caused by an interaction of the atoms with the oscillating electric field of the ambient thermal radiation. At an operating temperature of 300 K the shift is calculated to be -1.73×10^{-14} and varies as the fourth power of the absolute temperature [30].

4.1.4. Spin exchange frequency shift. Collisions between atoms travelling at different velocities inside the beam and with atoms in the background vapour pressure may cause an exchange of their electrons. This is called spin exchange and it creates a frequency shift proportional to the collision rate [9]. The collision rate is proportional to the relative velocities of the atoms and the collision cross section. The value of this cross section is not known for Cs at room temperature and the effect, although expected to be small, still needs to be evaluated.

4.2. Shifts introduced by the resonance detection system

4.2.1. Phase shift between the two cavities. If the phase shift Φ existing between the fields in the two arms forming the Ramsey cavity differs from either 0 or π by a small amount ϕ,

the central fringe is distorted, and its maximum or minimum is displaced. This phase shift may be caused by an asymmetry in the cavity construction creating a travelling wave within the structure. It may be thought of as a residual first-order Doppler effect. For monokinetic atoms it is given by

$$\Delta\nu_\phi = -\frac{\phi}{2\pi T}. \tag{6}$$

For example, an asymmetry of 10^{-4} m between the length of the two arms of the Ramsey cavity gives a frequency shift of the order of 10^{-13}. The frequency shift changes sign with a reversal of the velocity. It can thus be determined experimentally by reversing the direction of the beam. However, a perfect retracing of paths in the beam is difficult. This characteristic coupled to the presence of distributed phase shift across the beam limits the accuracy of determination of this shift. Its determination is usually made to an accuracy slightly better than 10^{-14} [31]. The problem of transverse distributed phase shift can also be minimized through the use of so-called ring structures [32, 33]. In short commercial instruments, the frequency shift is larger since T is smaller. It may reach 1×10^{-12}.

4.2.2. Cavity pulling. The cavity tuning does not influence the resonance maximum much. This is due to the fact that the cavity Q is low and that the effect of stimulated emission in the cavity is also very small because of the small number of atoms in interaction [10]. In short caesium beam frequency standards where the resonance is less selective, the effect may be significant. However, efficient means of suppressing this cavity pulling exists [9].

4.2.3. Bloch–Siegert effect. The magnetic induction in the cavity may be thought of as linearly polarized radiation. A linearly polarized field may be decomposed into two counter-rotating fields. In the rotating frame approach, one component is seen as resonant with the atomic ensemble and the other rotating in the opposite direction is seen as having twice the resonance frequency. An elementary analysis shows that a frequency shift is introduced in the detection of the resonance frequency by this off-resonance component. This shift is called the Bloch–Siegert effect [34]. It is proportional to the ratio l/L of the beam tube and in laboratory standards of large size it is of the order of 5×10^{-15}.

4.2.4. Majorana transitions. If the constant magnetic field along the atomic beam is inhomogeneous, transitions of random nature can be caused between m_F sublevels of the two manifolds $F = 3$ and $F = 4$. These are called Majorana transitions [35]. It has been shown that these transitions can cause a shift of the resonance frequency of the central $\Delta m_F = 0$ transition [4, p 427]. Since in the classical approach the selector magnet may cause those stray fields it is possible that such shifts exist in these devices. Special care is generally taken to avoid this effect by trimming the leakage field appropriately when necessary [36]. This effect is absent in optically pumped beam tubes where the magnetic field can be made sufficiently homogeneous all along the beam path.

4.2.5. Rabi and Ramsey frequency pulling. This is an effect that is partly inherent to the atoms and partly introduced through the technique of detection of the resonance. A shift is introduced by the overlapping of the symmetrically situated field-dependent Rabi pedestals with the central fringe of the $\Delta F = 1$, $\Delta m_F = 0$ resonance line [37–39]. When these pedestals have different amplitudes, which is the case for magnetic state selection, a small distortion of the central fringe is created by the tails of the field-dependent Rabi pedestals, causing a frequency shift of the central fringe. Furthermore, the microwave field in the cavity may contain a small perpendicular component causing transitions $\Delta F = 1$, $\Delta m_F = \pm 1$ that are connected to the resonant transition of interest by a common energy level. These transitions may also distort the central fringe and cause a small frequency shift. This is called Ramsey pulling. These shifts are a function of beam design and depend to some extent on the microwave power applied to detect the resonance. The effect is a function of the magnetic field applied and is smaller the narrower the resonance line. Consequently, these effects are much reduced in laboratory standards. A considerable amount of theoretical analysis has been done on these effects, and they are still under evaluation [40, 41].

4.2.6. Microwave leakage. An undesired microwave field may be present all around the microwave cavity when microwave leakage occurs. The spurious field may originate from the atomic beam holes or from a slit between different parts of the cavity assembly. It may also originate from electrical feedthroughs or may find its way through the optical windows in optically pumped set-ups. The atomic beam may then be subjected to a travelling wave in a place where no microwave field should be present. A Doppler frequency shift then occurs. A model of this effect has been presented, which accounts for the frequency shifts that may be observed [42].

4.2.7. Light shift. In early development stages it was believed that in the case of the optical pumping approach, the fluorescence emitted in the pumping region could cause a frequency shift known as a light shift [43], through diffusion to the microwave cavity. This light shift can be calculated and evaluated experimentally. It is found that in properly designed systems it is small and does not affect the accuracy of the standard at the present level of accuracy achieved [44–47].

4.2.8. Gravitational effect. According to the general theory of relativity clock rate is a function of the gravitational potential at the location of the clock. Consequently, the atomic Cs standard frequency is a function of its altitude in the Earth's field. Since the laboratory Cs beam frequency standards used in the determination of the SI second are located at different altitudes, it is thus important to precisely determine the actual altitudes of these standards relative to the geoid and make the appropriate correction [12]. This shift is small and is equal to $(gh/c^2) \times \nu_{hf}$, where g is the acceleration due to gravity at the location of the clock, h its altitude relative to the geoid and c is the speed of light. The fractional effect on the frequency is 10^{-16} per metre. The uncertainty in the determination of this shift is negligible.

4.3. Offsets introduced by the electronic servo system

4.3.1. Spectrum of the microwave radiation. Imperfections in the spectrum of the microwave radiation and in its modulation can cause frequency shifts [48]. The microwave radiation at 9.2 GHz is normally obtained by synthesis from a quartz crystal oscillator at a nominal frequency, say of 10 MHz. The process generally creates sidebands at various frequencies and furthermore amplifies any spurious spectral components present in the spectrum of the quartz crystal oscillator. These sidebands create virtual transitions in the atomic beam and cause frequency shifts [48].

4.3.2. Modulation and demodulation related frequency shifts. These shifts are related to distortion of the modulation and demodulation signals that are used in the creation of the error signal by the synchronous detection process [9, 10]. Even harmonics in the spectrum cause frequency shifts. Distortion ratios less than 10^{-6} are preferable to make the effects negligible at the level of accuracy encountered in state-of-the-art standards.

4.3.3. Frequency control loop. Finite dc gain in the control loop and voltage offsets can cause frequency offsets in the frequency lock loop. In state-of-the-art designs, digital servo loops are used and such offsets are eliminated [49–52].

5. Frequency stability

The frequency stability of the Cs beam frequency standard depends on the averaging time and on several factors, such as the modulation and frequency locking scheme. In the so-called short term region where shot noise at the beam detection is important, the frequency stability is given approximately by [9]

$$\sigma(\tau) = \frac{k'}{Q_l (S/N) \tau^{1/2}}, \tag{7}$$

where Q_l is the atomic line Q, S/N is the signal to noise ratio limited by shot noise at the detector, k' is a factor close to unity and τ is the averaging time. The range of application of this equation depends on the servo loop, integrating filter type and bandwidth. As an example, in some well-designed laboratory standards using magnetic state selection a frequency stability of $5 \times 10^{-12}\tau^{-1/2}$ over a range extending to 40 days has been measured, in general agreement with the above expression [24]. The best medium term frequency stability achieved with a laboratory optically pumped frequency standard is $3.8 \times 10^{-13}\tau^{-1/2}$ [16].

The long term frequency stability of Cs beam frequency standards depends on the stability of the various frequency shifts and offsets enumerated earlier. Consequently, the frequency of a unit is dependent to a certain extent on its environment. Temperature, humidity, atmospheric pressure and magnetic field, depending on construction, play roles, to various degrees, in determining long term frequency stability. Temperature fluctuations appear to have the most important effect. In general, best results are obtained in a temperature-controlled environment.

Fluctuations of unknown origins generally limit the frequency stability in the long term. When the averaging time τ is increased, the frequency stability as given by equation (7) improves and reaches a plateau called the flicker floor. The level of this flicker floor is a function of several parameters, generally unknown. Better quality in construction and design lowers this flicker floor to nearly undetectable levels.

6. State-of-the-art accuracy and frequency stability

As mentioned in the introduction, several national institutions engaged in primary standards work have implemented versions of the Cs beam standards described earlier. This work has spanned a period of over 50 years. It would not be possible to give appropriate credit to all those who have contributed by original ideas and have made the field progress to the stage it is at today. It should also be mentioned that several institutions are still actively involved in assessing new ways of evaluating the various effects causing frequency shifts and offsets as well as understanding better basic phenomena taking place in the operation of such standards. In fact, it is only through such activities that confidence is established in our accurate implementation of the definition of the SI unit, the second.

The size of the various offsets described above is summarized in table 1 along with present state-of-the-art accuracy in the determination of these offsets. The table is given without reference to particular units implemented and is given solely as a guide to the reader as to the relative importance of a given shift and how accurately it can be determined in best experimental conditions. At present, it appears that the biggest shift is the magnetic field offset. However, it is felt that the accuracy with which it is determined does not cause a major problem if care is taken in the design of the magnetic environment. The greatest cause of inaccuracy is probably still the cavity distributed phase shift limiting the accuracy to which the phase asymmetry in the Ramsey cavity can be determined.

It thus appears that the laboratory Cs beam frequency standard field has reached a high level of maturity. This stage has been attained through intensive research and development, construction of more sophisticated units, better understanding of the fundamental phenomena taking place and collaboration between the institutions. Table 2 is a compilation of the main characteristics of several laboratory units that have been developed in various institutions and have played and, in some cases, still play an important role in the accuracy of TAI. Most of them have been influential in the design of the following primary standards.

The main characteristics of the most recently developed primary frequency standards are given in table 3. In most cases, they show an improvement in both frequency stability and accuracy of an order of magnitude over the standards listed in table 2. They appear to have reached such a level of accuracy that improvements can only be made at substantial costs and efforts although, as in the case of Rabi and Ramsey pulling, a better theoretical understanding of the effect may lead to a somewhat improved accuracy in its determination.

7. Other developments

In order to avoid problems related to the Rabi and Ramsey pulling effects mentioned above, an approach using optical pumping of a Cs atomic beam but operating in a high magnetic

Table 1. Order of magnitude of bias or offsets present in laboratory Cs beam frequency standards. The uncertainty given is that achieved in the best circumstances and is given as a reference to the accuracy that may be achieved in practice.

Origin of bias or offset	Typical size in laboratory standards (parts in 10^{-15})	Typical smallest evaluation uncertainty achieved (parts in 10^{-15})
Magnetic field	>100 000	0.1
Second-order Doppler effect	Depends on construction $> \lvert-50\rvert$	1
Black body radiation	∼20	0.3
Spin exchange interactions	unknown	Expected ⩽1
Cavity phase shift	>100 depends on construction	1 to 10
Cavity pulling	∼5 to 10	0.6
Bloch–Siegert effect	∼1	Expected ⩽0.3
Majorana transitions	∼2	<1.3
Rabi and Ramsey pulling	<2	0.02
Microwave spectrum	<1	0.1
Electronics, mod., demod., etc	1	1
Microwave leakage	Depends on construction	<1
Gravitation	Depends on location	<0.1
Fluorescence light shift	<2	<0.5

Table 2. Characteristics of selected laboratory primary frequency standards developed in the 1970s and 1980s.

	NRC (Canada) Cs V	NRC (Canada) Cs VI A & C	GOSSTRDT (USSR) MCs R 101	GOSSTRDT (USSR) MCs R 102	NIST (USA) NBS 6	CRL (Japan) Cs1	NRLM (Japan) NRLM II	NIM (China) Cs2
Distance between Ramsey cavities/m	2.1	1	0.65	1	3.7	0.55	1	3.68
Microwave-magnetic field direction/beam	⊥	⊥	⊥	=	⊥	⊥	⊥	
State selector-analysers	2 poles	2 poles	2 poles	hexapole	2 poles	hexapole	2 poles	2 poles
Mean atom velocity/(m s^{-1})	250	200	170–220	220	195	110	300	
Line width/Hz	60	100	130–200	110	26	100	150	
$\sigma_y(\tau)\tau^{+1/2}$	3×10^{-12}	3×10^{-12}	3×10^{-12}	5×10^{-12}	2×10^{-12}	5×10^{-12}	$<8 \times 10^{-12}$	1.8×10^{-11}
Accuracy	1×10^{-13}	1×10^{-13}	1×10^{-13}	5×10^{-14}	9×10^{-14}	1.1×10^{-13}	2.2×10^{-13}	4.1×10^{-13}
Reference	Mungall *et al* (1973, 1977) [76, 77]	Mungall *et al* (1981) [20]	Abaschev *et al* (1983, 1987) [78, 79]	Abaschev *et al* (1983, 1987) [78, 79]	Lewis *et al* (1881) [80]	Nagakiri *et al* (1981, 1987) [81, 82]	Koga *et al* (1981) [83], Nakadan *et al* (1982) [84]	Xiaoren (1981) [85]

field has been proposed [53]. In that case, the transition $F = 4$, $m_F = -1$ to $F = 3$, $m_F = -1$ is used at a magnetic induction of 82 mT. In such a field, the transition frequency is minimized and equal to $(15/16)^{1/2}\nu_{hf}$ with a quadratic field dependence. An evaluation of the various sources of bias shows that an accuracy of the order of 10^{-14} should, in principle, be possible, although it appears that in practice problems involved with the homogeneity and stability of the high magnetic field required remain a major challenge. Nevertheless, solutions to these practical problems are being studied [53].

Another approach using stimulated-resonance Raman interaction in a beam has also been proposed [54]. The technique consists in applying laser radiation to two regions or zones of an alkali atomic beam, separated by a distance L. The laser radiation consists of two radiation fields at frequencies ω_1 and ω_2 forming a so-called Λ scheme, applied to each zone at right angles to the beam propagation, and connecting the two atomic hyperfine levels of the ground state to a common excited state. Such an excitation has also been called coherent population trapping (CPT). When the frequency difference $\omega_{12} = (\omega_1 - \omega_2)$ of the two radiation fields is equal to the ground state hyperfine frequency, the atomic ensemble in interaction with the radiation is placed in a so-called dark state and a coherence is created in the ground state at that particular frequency ω_{12}. The coherence created in the first zone is carried by the beam of atoms into the second zone of interaction, separated from the first one by the distance L. Memory of the phase established in the first zone is kept downstream by the atoms and interference takes place in the second zone. The phenomenon is detected directly on the fluorescence emitted by those atoms in the beam that are in interaction with the laser radiation fields in the second zone. The interference leads to Ramsey fringes similar to those observed in the classical approach. The main difference lies in the absence of the microwave Ramsey cavity, the Raman excitation acting essentially as a $\pi/2$ pulse. In its early stages, the concept was implemented on a sodium beam using a dye laser [54]. It was later adapted to a caesium beam using laser diodes [55]. Studies have been made both experimentally and theoretically on the signal amplitude and shape, on frequency shifts and on phase shifts that may be present in such a system due to the ac Stark effect or light shift [56, 57]. The

Table 3. Characteristics of several recently constructed primary frequency standards that show a high level of frequency stability and accuracy.

	PTB (Germany) Cs 1	PTB (Germany) Cs 2	PTB (Germany) Cs 3	SYRTE (France) JPO	NIST (USA) NIST-7	NIICT (Japan) CRL-01 (NICT01)	NRLM (Japan) NRLM-4
Distance between Ramsey cavities/m	0.8	0.8	0.77 (vertical construction)	1.03	1.53	1.53	0.96
Microwave-magnetic field direction/beam	=	=	=	$\perp$	=	=	$\perp$
State selector-analysers	Hexapole+ quadrupole	Hexapole+ quadrupole	hexapole	Optical pumping: selection: $F = 4$–$F' = 4$ detection: $F = 4$–$F' = 5$	Optical pumping: selection: $F = 4$–$F' = 3$ detection: $F = 4$–$F' = 5$	Optical pumping: selection: $F = 4$–$F' = 3$ detection: $F = 4$–$F' = 5$	Optical pumping: selection: $F = 4$–$F' = 4$ detection: $F = 4$–$F' = 5$
Mean atom velocity/(m s^{-1})	93	93	72	215	230	250	
Line width/Hz	59	60	44	100	77	62	100
$\sigma_y(\tau)\tau^{+1/2}$	5×10^{-12}	4×10^{-12}	9×10^{-12}	3.5×10^{-13}	1×10^{-12}	3×10^{-12}	$(7–9) \times 10^{-13}$
Accuracy	7×10^{-15}	12×10^{-15}	1.4×10^{-14}	6.4×10^{-15}	5×10^{-15}	6.8×10^{-15}	2.9×10^{-14}
Reference	Bauch *et al* (1998, 2003) [31, 86]	Bauch *et al* (2003) [31]	Bauch *et al* (1996) [87]	Makdissi *et al* (2001) [47]	Shirley *et al* (2001) [44]	Hasegawa *et al* (2004) [88]	Hagimoto *et al* (1999) [45]

approach has many interesting features relative to size and simplicity of construction. However, no work appears to have been pursued up to the present in using CPT in an atomic beam approach, although intensive work initiated in the 1990s [58, 59] is being done currently in the implementation of small frequency standards based on the CPT phenomenon in sealed cells using a buffer gas [60–64].

Several institutions throughout the world have engaged recently in efforts to develop their own primary room temperature Cs beam frequency standards of the classical type. However, in some cases, the effort is somewhat modest in view of the greater interest raised by recent developments in atom laser cooling that led to the development of the atomic fountain, providing a better frequency stability and accuracy. In this context, it is worth mentioning efforts in Brazil [65] and in Korea [26, 41], where optically pumped standards are being developed and are still under evaluation.

8. Commercial Cs beam frequency standards

Commercial Cs beam frequency standards form the subject of another publication in this special issue [66]. Consequently, the following discussion will be very concise and the reader is referred to that publication for more details.

The industrial development of commercial Cs beam frequency standards started in the USA at the National Company with the assistance of Professor Zacharias following research and development at the Massachusetts Institute of Technology [67]. The National Company 'Atomichron' Model 2001 was the first commercial atomic clock [68]. It was of vertical construction, 2 m high, had a frequency stability of 5×10^{-11} for an averaging time of 1 s and had a specified accuracy of 5×10^{-11}. Development of more advanced compact frequency standards followed the work of Holloway at the National Company, at Varian Associates and at Hewlett–Packard now Agilent [69].

Commercially available Cs beam frequency standards are currently designed using magnetic state selection and a Ramsey interaction structure of the order of 20 cm in length. Since they cannot be evaluated as thoroughly as laboratory standards they are not generally considered as primary standards. However, in some cases, the standard construction is such as to provide a relatively high level of accuracy. For example, it is possible to adjust the magnetic induction in a short tube so as to make the Rabi and Ramsey offsets, as well as the microwave power sensitivity, negligible [10]. An accuracy of 10^{-12} has been claimed in specially selected units [70]. A reproducibility of 5×10^{-13} is also reported. Their typical frequency stability is $8.5 \times 10^{-12}\,\tau^{-1/2}$ in the range $10^4\,\text{s} < \tau < 30$ days with a flicker floor of about 1×10^{-14}.

Nowadays, commercially built Cs beam frequency standards are used in multiple applications demanding high frequency stability and reliability. These include, for example, digital communication systems and advanced navigation systems, such as the LORAN C, GPS and Glonass. A large number (hundred) of these units are used throughout the world by national institutes for maintaining their time scales. They are part of atomic clock ensembles incorporating several standards such as H masers and classical laboratory primary standards operating continuously. The information obtained is transmitted to the BIPM for the implementation of the International Atomic Time scale TAI, while the SI unit size is maintained by large primary standards in national standards institutions [71].

At the time of writing, no commercial Cs beam tubes using the optical pumping state selection approach are available, although relatively large laboratory effort has been deployed and frequency stability figures of about $(1–3) \times 10^{-12}\,\tau^{-1/2}$ have been obtained [72–74]. A simplified design, based on an optically pumped beam travelling along the axis of a TE_{012} cylindrical cavity has also been evaluated [75].

9. Conclusion

In this paper, we have reviewed the state of the art of the classical atomic Cs beam frequency standard operating at room temperature. We have described approaches using both magnetic and optical pumping state selection and have given an outline of the progress accomplished over 50 years of its intensive development. The main bias and offsets that affect the accuracy of that type of frequency standard were described and the present state of the art in the understanding and analysis of these offsets was outlined, with a review of the level of accuracy reached. It appears that the best accuracy is currently achieved with optical pumping state selection although a magnetic state selection giving preference to a beam of low velocity atoms has attained a similar accuracy. An accuracy of the order of (5–7) $\times 10^{-15}$ has been reached. The frequency stability achieved in well-designed units reaches 3.5×10^{-13} for an averaging time of 1 s. At present, the uniformity of the international atomic time scale TAI as maintained at the BIPM relies mainly on commercial Cs beam clocks while its accuracy is ensured to some extent by means of primary standards of the type mentioned above in table 3.

We may finally conclude by saying that the field of passive Cs beam frequency standards has reached a high level of maturity. It appears that improvements, although still possible, will require significant efforts to understand better some of the phenomena affecting their accuracy, such as the Ramsey–Rabi pulling. It also appears that improvements in the future will have to rely on new avenues such as atom laser cooling.

References

[1] Essen L and Parry V I 1955 *Nature* **176** 280–4
[2] Ramsey N F 1950 *Phys. Rev.* **78** 695–9
[3] Conférence générale des poids et mesures 1967–68 Resolution 1, CR, 103
Terrien J 1968 *Metrologia* **4** 41–5
[4] Ramsey N F 1956 *Molecular Beams* (Oxford: Clarendon)
[5] Rabi I I, Zacharias J R, Millman S and Kush P 1938 *Phys. Rev.* **53** 318
[6] Kush P, Millman S and Rabi I I 1940 *Phys. Rev.* **57** 765–80
[7] Gerlach W and Stern O 1924 *Ann. Phys., Lpz.* **74** 673
Gerlach W and Stern O 1925 *Ann. Phys., Lpz.* **76** 163
[8] Kastler A J 1950 *Phys. Radium* **11** 255–65
[9] Vanier J and Audoin C 1989 *The Quantum Physics of Atomic Frequency Standards* (Bristol: Hilger)
[10] Audoin C 1992 *Metrologia* **29** 113–34
[11] Vanier J 2001 Recent advances in metrology and fundamental constants *International School of Physics, 'Enrico Fermi', Course CXLVI* (Bologna: Societa Italiana di Fisica) ed T J Quinn *et al* pp 397–452
[12] Audoin C and Guinot B 2001 *The Measurement of Time* (Cambridge: Cambridge University Press)
[13] Arditi M and Cerez P 1972 *IEEE Trans. Instrum. Meas.* **21** 391–5
[14] Arditi M and Picqué J L 1980 *J. Physique Lett.* **41** L379–81
[15] Avila G, Giordano V, Candelier V, de Clercq E, Théobald G and Cérez P 1987 *Phys. Rev.* A **36** 3719–28
[16] Makdissi A, Berthet J P and de Clercq E 1997 *Proc. 11th European Frequency and Time Forum (Neuchâtel, Switzerland)* pp 564–6
[17] Dimarcq N, Giordano V, Cérez P and Théobald G 1993 *IEEE Trans. Instrum. Meas.* **42** 115–20
[18] Abragam A 1961 *The Principles of Nuclear Magnetism* (Oxford: Clarendon)
[19] Audoin C 1980 Metrology and fundamental constants *International School of Physics, 'Enrico Fermi', Course XXXX* (Bologna: Societa Italiana di Fisica) ed A Ferro-Milone and P Giacomo pp 223–59
[20] Mungall A G, Damms H and Boulanger J S 1981 *Metrologia* **17** 123–45
[21] Cérez P, Théobald G, Giordano V, Dimarcq N and de Labachelerie M 1991 *IEEE Trans. Instrum. Meas.* **40** 137–41
[22] Kobayashi M, Nagakiri K, Urabe S, Shibuki M and Saburi Y 1978 *IEEE Trans. Instrum. Meas.* **27** 343–8
[23] Audoin C, Giordano V, Dimarcq N, Cérez P, Petit P and Théobald G 1994 *IEEE Trans. Instrum. Meas.* **43** 515–20
[24] Bauch A, Fischer B, Heindorff T and Schröder R 1999 *Proc. Joint Meeting of the European Frequency and Time Forum/IEEE Int. Frequency Control Symp. (Besançon, France)* pp 43–6
[25] Lee H S, Park S E, Kwon T Y, Yang S H and Cho H 2001 *IEEE Trans. Instrum. Meas.* **50** 531–4
[26] Lee H S, Kwon T Y, Park S E and Choi S K 2004 *J. Korean Phys. Soc.* **45** 256–72
[27] Boulanger J S, Douglas R J, Vanier J, Mungall A G, Li Y S and Jacques C 1984 *Proc. 16th Ann. Precise Time and Time Interval (PTTI) Applications and Planning Meeting (Washington DC, 1984)* pp 59–80
[28] Boulanger J S 1986 *Metrologia* **23** 37–44
[29] Shirley J H 1997 *IEEE Trans. Instrum. Meas.* **46** 117–21
[30] Itano W N, Lewis L L and Wineland D J 1981 *J. Physique* **42** C8 283–7
[31] Bauch A, Schröder R and Weyers S 2003 *Proc. Joint Meeting 17th European Frequency and Time Forum/IEEE Int. Frequency Control Symp. and PDA Exhibition (Tampa, FL)* pp 191–9
[32] DeMarchi A 1986 *Proc. 40th Annual Frequency Control Symp. (Philadelphia, PA)* pp 441–6
[33] DeMarchi A, Shirley J H, Glaze D J and Drullinger R E 1988 *IEEE Trans. Instrum. Meas.* **37** 185–90
[34] Bloch F and Siegert A 1940 *Phys. Rev.* **57** 522–7
[35] Majorana E 1932 *Nuovo Cimento* **9** 43
[36] Bauch A and Schröder R 1993 *Ann. Phys., Lpz.* **2** 421–49
[37] DeMarchi A, Rovera G D and Premoli A 1984 *Metrologia* **20** 37–47
[38] DeMarchi A 1987 *IEEE Trans. Ultrason. Ferroelectr. Freq. Control* **34** 598–601
[39] Cutler L S, Flory C A, Giffard R P and DeMarchi A 1991 *J. Appl. Phys.* **69** 2780–92
[40] Shirley J H, Lee W D, Rovera G D and Drullinger R E 1995 *IEEE Trans. Instrum. Meas.* **44** 136–9
[41] Lee H S, Kwon T Y, Kang H-S, Park Y O, Oh C-H, Park S E, Cho H and Minogin V G 2003 *Metrologia* **40** 224–31
[42] Boussert B, Théobald G, Cérez P and de Clercq E 1998 *IEEE Trans. Ultrason. Ferroelectr. Freq. Control* **45** 728–38
[43] Barrat J P and Cohen-Tannoudji C 1961 *J. Physique Radium* **22** 329–43
Barrat J P and Cohen-Tannoudji C 1961 *J. Physique Radium* **22** 443–50
[44] Shirley J H, Lee W D and Drullinger R E 2001 *Metrologia* **38** 427–58
[45] Hagimoto K, Oshima S, Nakadan Y and Koga Y 1999 *IEEE Trans. Instrum. Meas.* **48** 496–9
[46] Makdissi A and de Clercq E 2000 *IEEE Trans. Ultrason. Ferroelectr. Freq. Control* **47** 461–5
[47] Makdissi A and de Clercq E 2001 *Metrologia* **38** 409–25
[48] Audoin C, Jardino M, Cutler L S and Lacey R F C 1978 *IEEE Trans. Instrum. Meas.* **27** 325–9
[49] Nakadan Y and Koga Y 1985 *IEEE Trans. Instrum. Meas.* **34** 133–5
[50] Garvey R M 1982 *Proc. 36th Annual Frequency Control Symp. (Philadelphia, PA)* pp 236–9
[51] Rabian J and Rochat P 1988 *Proc. 2nd European Frequency and Time Forum (Neuchâtel, Switzerland)* pp 461–8

[52] Sing L T, Viennet J and Audoin C 1990 *IEEE Trans. Instrum. Meas.* **39** 428–9
[53] Costanzo A G, Siccardi M, Barychev V and De Marchi A 2000 *IEEE Trans. Ultrason. Ferroelectr. Freq. Control* **47** 249–55
[54] Thomas J E, Hemmer P R, Ezekiel S, Leiby C C Jr, Picard R H and Willis C R 1982 *Phys. Rev. Lett.* **48** 867–70
[55] Hemmer P R, Shahriar M S, Lameal-Rivera H, Smith S P, Bernacki B E and Ezekiel S 1993 *J. Opt. Soc. Am.* B **10** 1326–9
[56] Hemmer P R, Shahriar M S, Natoli V D and Ezekiel S 1989 *J. Opt. Soc. Am.* B **6** 1519–28
[57] Kim J Y and Cho D 2000 *J. Korean Phys. Soc.* **37** (part 2) 745–50
[58] Cyr N, Têtu M and Breton M 1993 *IEEE Trans. Instrum. Meas.* **42** 640–9
[59] Vanier J, Godone A and Levi F 1998 *Phys. Rev.* A **58** 2345–58
[60] Godone A, Levi F and Vanier J 1999 *Phys. Rev*. A **59** R12–15
[61] Vanier J, Levine M, Kendig S, Janssen D, Everson C and Delaney M 2004 *Proc. IEEE Int. Ultrason. Ferroelectr./ Frequency Control, Joint 50th Anniversary Conf. (Montreal, Canada)* pp 92–9
[62] Merimaa M, Lindvall T, Tittonen I and Ikonen E 2003 *J. Opt. Soc. Am.* B **20** 273–9
[63] Liew L-A, Knappe S, Moreland J, Robinson H, Hollberg L and Kitching J 2004 *Appl. Phys. Lett.* **84** 2694–6
[64] Zanon T, Tremine S, Guerandel S, De Clercq E, Holleville D, Dimarcq N and Clairon A 2005 *IEEE Trans. Instrum. Meas.* **54** 776–9
[65] Teles F, Magalhaes D V, Santos M S, Bebeachibuli A and Bagnato V S 2002 *Metrologia* **39** 135–41
[66] Cutler L S 2005 *Metrologia* **42** S90–9
[67] Zacharias J R, Yates J G and Haun R D 1955 *Proc. IRE* **43** 364
[68] Mainberger W A 1958 *Electronics* **31** 80
[69] McCoubrey A and Cutler L 1972 *Proc. 26th Ann. Symp. on Frequency Control (Springfield, VA, National Technical Information Service)* p 202
[70] Hewlett-Packard (now Agilent) 1992 *Spec Sheet on HP 5071 Primary Frequency Standard*
[71] Thomas C 1997 *IEEE Trans. Ultrason. Ferroelectr. Freq. Control* **44** 693–700
[72] Guérandel S, Hermann V, Barillet R, Cerez P, Théobald G, Audoin C, Chassagne L, Sallot C and Delporte J 2002 *Proc. IEEE Int. Frequency Control Symp. and PDA Exhibition (New Orleans, LA)* pp 480–3
[73] Lutwak R, Emmons D, Garvey R M and Vlitas P 2001 *Proc. 33rd Annual Precise Time and Time Interval (PTTI) Systems and Applications Meeting (Long Beach, CA)* pp 19–32
[74] Sallot C, Baldy M, Gin D and Petit R 2003 *Proc. Joint Meeting 17th European Frequency and Time Forum/IEEE Int. Frequency Control Symp. and PDA Exhibition (Tampa, FL)* pp 100–4
[75] Hermann V, Guérandel S, Audoin C, Barillet R, Cérez P and Théobald G 2003 *Proc. Joint Meeting 17th European Frquency and Time Fourm/IEEE Int. Frequency Control Symp. and PDA Exhibition (Tampa, FL)* pp 37–40
[76] Mungall A G, Bailey R, Daams H, Morris D and Costain C C 1973 *Metrologia* **9** 113–27
[77] Mungall A G and Costain C C 1977 *Metrologia* **13** 105–7
[78] Abaschev Y G, Elkin G A and Pskin S B 1983 *Izmeritel'naya Tekhnika* **12** 36–8
[79] Abaschev Y G, Elkin G A and Pskin S B 1987 *IEEE Trans. Instrum. Meas.* **36** 627–9
[80] Lewis L L, Walls F L and Glaze D J 1981 *J. Physique* **42** C8 241–6
[81] Nagakiri K, Shibuki M, Uabe S, Hayashi R and Saburi Y 1981 *J. Physique* **42** C8 253–6
[82] Nagakiri K, Shibuki M, Okazawa H, Umezu J, Ohta Y and Saitoh H 1987 *IEEE Trans. Instrum. Meas.* **36** 617–19
[83] Koga Y, Nakadan Y and Yoda J 1981 *J. Physique* **42** C8 247–52
[84] Nakadan Y and Koga Y 1982 *Proc. 36th Annual Frequency Control Symp. (Philadelphia, PA)* pp 223–9
[85] Xiaoren Y 1981 *J. Physique* **42** C8 257–60
[86] Bauch A, Fischer B, Heindorff T and Schröder R 1998 *Metrologia* **35** 829–45
[87] Bauch A, Heindorff T, Schröder R and Fischer B 1996 *Metrologia* **33** 249–59
[88] Hasegawa A, Fukuda K, Kajita M, Ito H, Kumagai M, Hosokawa M, Kotabe N and Morikawa T 2004 *Metrologia* **41** 257–63